Theoretical description of the fourth-forbidden non-unique β decays of ^{113}Cd and ^{115}In

M. T. Mustonen, M. Aunola, and J. Suhonen
Department of Physics, University of Jyväskylä, P.O. Box 35, FIN-40351 Jyväskylä, Finland
(Received 25 January 2006; published 3 May 2006)

The half-lives and log ft values for the fourth-forbidden non-unique beta decays of the ground states of ^{113}Cd and ^{115}In were calculated using a transparent formulation for the β^- transition amplitude. The microscopic quasiparticle-phonon model (MQPM) was used to calculate the initial and final states of the transitions. The corresponding wave functions were described as linear combinations of one- and three-quasiparticle configurations built in a realistic single-particle model space by using a realistic microscopic two-body interaction. The computed results for the log ft values and half-lives are reasonably close to the available experimental data.

DOI: 10.1103/PhysRevC.73.054301 PACS number(s): 21.60.Jz, 23.40.Hc, 27.60.+j

I. INTRODUCTION

The fourth-forbidden non-unique beta decays have log ft values larger than 20 and half-lives around 10^{15} years. Only three isotopes having only this decay channel open are currently known: ^{50}V, ^{113}Cd, and ^{115}In [1]. There are, however, highly-forbidden beta-decay transitions, e.g., in the decays of ^{48}Ca and ^{96}Zr which also decay by the double beta decay (see, e.g., Ref. [2]). In these nuclei the decay Q value allows the 0^+ ground state to decay to the 4^+ (fourth-forbidden non-unique), 5^+ (fourth-forbidden unique), and 6^+ (sixth-forbidden non-unique) states in the daughter nuclei ^{48}Sc and ^{96}Nb. The decay of ^{48}Ca was previously treated by using the nuclear shell model in Ref. [3].

The microscopic quasiparticle-phonon model (MQPM) [4] was developed to describe states of open-shell odd-A nuclei [5]. Thus it is suited to study of the decays of ^{113}Cd and ^{115}In. For both of these decays some experimental data exists: in addition to the half-lives, log ft values and the excitation spectra evaluated in Refs. [6,7], there is also a very recent measurement for the half-life of ^{113}Cd [1]. These data have been collected in Fig. 1.

The kinematical part of beta decay is well established in literature (e.g., in Ref. [8]). In the present work we apply the formulation of Ref. [8] for the non-unique β^- decays by giving explicit expressions for the involved shape functions and nuclear matrix elements. Calculation of the single-particle matrix elements and the nuclear matrix elements makes use of our explicitly written charge-changing transition densities, which have to be computed by using a nuclear model. For the presently discussed odd-mass nuclei the needed transition densities are easily computed using the formalism of the MQPM [4].

The MQPM provides an internally consistent, fully microscopic way of describing spherical (or nearly spherical) open-shell odd-A nuclei. The same nucleon-nucleon interaction is used all the way from generating the quasiparticles and phonons to coupling them to three-quasiparticle configurations. Thus far only allowed beta decays have been considered in the MQPM framework, e.g., in Ref. [4] and [9]. However, since the forbiddeness of the beta decay does not affect the description of the initial and final nuclear states, the MQPM computed transition densities just have to be implemented in the general beta-decay framework of Ref. [8]. Still, the computation of the log ft values for non-unique forbidden decays takes a lot more effort than for the allowed or unique-forbidden decays as there are either four (second-forbidden and higher) or six (first-forbidden) nuclear matrix elements to be considered, instead of just one or two. Non-unique first-forbidden beta decay was discussed earlier in Refs. [10–12] for odd-odd mother nuclei.

This article is organized as follows. In Sec. II we give the necessary theoretical background on the MQPM and non-unique forbidden beta decay. In Sec. III we apply the reviewed formalism to compute beta-decay log ft values and half-lives for the ^{113}Cd and ^{115}In decays. In Sec. IV we summarize our results and draw the conclusions.

II. THEORETICAL BACKGROUND

A. Microscopic quasiparticle-phonon model

In the BCS approach [13] the ground state of an even-even nucleus is described as a superconducting medium where all the nucleons have formed pairs that effectively act as bosons. Formally the BCS ground state is defined as

$$|\mathrm{BCS}\rangle = \prod_{\alpha>0}(u_a - v_a c^\dagger_\alpha \tilde{c}^\dagger_\alpha)|\mathrm{CORE}\rangle, \tag{1}$$

where $|\mathrm{CORE}\rangle$ represents the nuclear core (effective particle vacuum), $c^\dagger_\alpha$ is the particle creation operator and u_a and v_a are the unoccupation and occupation amplitudes, which are to be determined. The notation of Baranger [14] is adopted here for the quantum numbers of the single-particle states: the Roman letter a includes the quantum numbers n_a, l_a and j_a. The Greek letter α includes all the quantum numbers of a and the magnetic quantum number m_α. The notation $\alpha > 0$ is interpreted as $m_\alpha > 0$. The time-reversed operator has been defined as $\tilde{c}^\dagger_\alpha = (-1)^{j_a+m_a} c^\dagger_{-\alpha}$, where $-\alpha = \{a, -m_\alpha\}$.

The BCS ground state (1) acts as a vacuum for quasiparticles. The creation and annihilation operators for quasiparticles are constructed via the Bogolyubov-Valatin quasiparticle transformation: $a^\dagger_\alpha = u_a c^\dagger_\alpha + v_a \tilde{c}_\alpha$, $a_\alpha = u_a c_\alpha + v_a \tilde{c}^\dagger_\alpha$. The BCS quasiparticles satisfy the anticommutation relation $\{a^\dagger_\alpha, a_\beta\} = \delta_{\alpha\beta}$ and are therefore fermions.

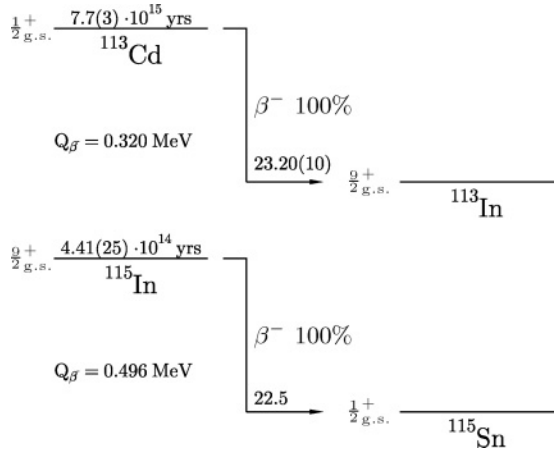

FIG. 1. Experimental data [6,7] on the decays of the ground states of ^{113}Cd and ^{115}In.

The occupation and unoccupation amplitudes can be solved by applying a variational procedure for minimizing the energy of the BCS ground state for protons and neutrons separately. Since the BCS ground state (1) lacks good particle number the variation is constrained by requiring the average proton and neutron numbers in the BCS ground state to correspond to the ones of the even-even nucleus under discussion.

After the quasiparticle transformation the nuclear Hamiltonian can be written in the form

$$H = H_{11} + H_{20} + H_{02} + H_{22} + H_{31} + H_{13} + H_{40} + H_{04}, \tag{2}$$

where each term is proportional to a normal-ordered product of creation and annihilation operators, i.e.,

$$H_{nm} \propto a^\dagger_{\alpha_1} \cdots a^\dagger_{\alpha_n} a_{\beta_1} \cdots a_{\beta_m}. \tag{3}$$

It turns out that when minimizing the ground-state energy with the variational procedure, the terms H_{20} and H_{02} vanish. This means that the quasiparticle transformation dumps a large part of the short-range residual interaction in noninteracting quasiparticles.

In practice, in the BCS calculations the monopole interaction matrix elements are often scaled so that the experimental pairing gaps are reproduced. The notation for these phenomenological scaling constants used here is $g^{(\mathrm{p})}_{\mathrm{pair}}$ for protons and $g^{(\mathrm{n})}_{\mathrm{pair}}$ for neutrons. The pairing gaps can be extracted from experimental data by using the linear approximation formulas [15]

$$\Delta_{\mathrm{p}}\left({}^{\mathrm{A}}_{\mathrm{Z}}\mathrm{X}\right) = \tfrac{1}{4}(-1)^{\mathrm{Z}+1}\left(S_{\mathrm{p}}\left({}^{\mathrm{A}+1}_{\mathrm{Z}+1}\mathrm{X}\right) - 2S_{\mathrm{p}}\left({}^{\mathrm{A}}_{\mathrm{Z}}\mathrm{X}\right) + S_{\mathrm{p}}\left({}^{\mathrm{A}-1}_{\mathrm{Z}-1}\mathrm{X}\right)\right) \tag{4a}$$

and

$$\Delta_{\mathrm{n}}\left({}^{\mathrm{A}}_{\mathrm{Z}}\mathrm{X}\right) = \tfrac{1}{4}(-1)^{\mathrm{A}-\mathrm{Z}+1}\left(S_{\mathrm{n}}\left({}^{\mathrm{A}+1}_{\mathrm{Z}}\mathrm{X}\right) - 2S_{\mathrm{n}}\left({}^{\mathrm{A}}_{\mathrm{Z}}\mathrm{X}\right) + S_{\mathrm{n}}\left({}^{\mathrm{A}-1}_{\mathrm{Z}}\mathrm{X}\right)\right), \tag{4b}$$

where $S_{\mathrm{n}}({}^{\mathrm{A}}_{\mathrm{Z}}\mathrm{X})$ and $S_{\mathrm{p}}({}^{\mathrm{A}}_{\mathrm{Z}}\mathrm{X})$ are the neutron and proton separation energies of the ${}^{\mathrm{A}}_{\mathrm{Z}}\mathrm{X}$ nuclide, respectively.

The logical next step in the quasiparticle framework is to consider the two-quasiparticle excitations, and hence, the terms H_{22}, H_{40}, and H_{04} of the residual interaction (2). This can be done via the quasiparticle random phase approximation (QRPA) [14]. The QRPA excitations—or *phonons*—are created with the operator

$$Q^\dagger_\omega = \sum_{a \leqslant a'} \left[X^\omega_{aa'} A^\dagger_{aa'}(J_\omega M) - Y^\omega_{aa'} \tilde{A}_{aa'}(J_\omega M)\right], \tag{5}$$

where ω stands for the angular momentum J_ω, the parity π_ω and the additional index k_ω which identifies the different excitations with the same angular momentum and parity. The summation is restricted so that double counting of pairs is avoided. The two-quasiparticle creation and annihilation operators are defined as $A^\dagger_{ab}(J_\omega M) = (1+\delta_{ab}(-1)^J)^{-1/2}[a^\dagger_a a^\dagger_b]_{J_\omega}$ and its time-reversed hermitian conjugate $\tilde{A}_{ab}(J_\omega M) = (-1)^{J_\omega - M} A_{ab}(J_\omega, -M)$. The X and Y amplitudes can be solved from the QRPA matrix equation, see, e.g., Ref. [16].

The simplest way to describe the states of an odd-A nucleus in the quasiparticle picture is to consider only the states where one quasiparticle is created on the BCS vacuum (the ground state of the even-even reference nucleus). To improve this description however, three-quasiparticle excitations should be included. The MQPM is a fully microscopic way to introduce the three-quasiparticle correlations and, consequently, to take the last two residual interaction terms of Eq. (2), namely, H_{31} and H_{13}, into account.

The MQPM excitation operator is written as

$$\Gamma^\dagger_i(jm) = \sum_n C^i_n a^\dagger_{njm} + \sum_{a\omega} D^i_{a\omega}[a^\dagger_a Q^\dagger_\omega]_{jm}, \tag{6}$$

where the amplitudes C^i_n and $D^i_{a\omega}$ are now to be determined. Use of the methods of Ref. [16] leads to a generalized eigenvalue equation

$$\begin{pmatrix} \mathbf{A} & \mathbf{B} \\ \mathbf{B}^{\mathrm{T}} & \mathbf{A}' \end{pmatrix} \begin{pmatrix} \mathbf{C}^i \\ \mathbf{D}^i \end{pmatrix} = \Omega_i \begin{pmatrix} \mathbf{1}\ 0 \\ 0\ \mathbf{n} \end{pmatrix} \begin{pmatrix} \mathbf{C}^i \\ \mathbf{D}^i \end{pmatrix}, \tag{7}$$

where the submatrix $\mathbf{n}$ of the metric matrix is nondiagonal, as the three-quasiparticle basis states do not form an orthogonal set. Typically the set of the three-quasiparticle states also forms an overcomplete basis. The procedure to overcome this difficulty and to transform to an ordinary eigenvalue equation is described in more detail in Ref. [4]. In the procedure the submatrix $\mathbf{n}$ is diagonalized and a complete set of basis states is achieved by discarding the eigenstates with zero eigenvalue.

The charge-changing transition densities (CCTD) for the β^- decay in the MQPM framework are

$$(p\|[c^\dagger_{p'}\tilde{c}_{n'}]_L\|n) = \hat{L} u_p u_n \delta_{pp'}\delta_{nn'} \tag{8}$$

and

$$(n\|[c^\dagger_{p'}\tilde{c}_{n'}]_L\|p) = \hat{L} v_n v_p \delta_{nn'}\delta_{pp'}(-1)^{j_{n'}+j_{p'}+L} \tag{9}$$

for transitions between one-quasiparticle states, and

$$\begin{aligned}(\omega pj\|[c^\dagger_{p'}\tilde{c}_{n'}]_L\|n) = (-1)^{j_p+J_\omega-j}\hat{J}_\omega\hat{L}\hat{j}\Bigg[&\begin{Bmatrix} j_n & j & L \\ j_p & j_{n'} & J_\omega \end{Bmatrix} \\ &\times \bar{X}^\omega_{nn'} u_{p'} v_{n'} \sigma^{-1}_{nn'} \delta_{pp'}(-1)^{j_n+j+L} \\ &+ \frac{\delta_{jj_{p'}}}{\hat{j}^2}\bar{Y}^\omega_{pp'} v_{p'} u_{n'} \sigma^{-1}_{pp'}\delta_{nn'}\Bigg]\end{aligned} \tag{10}$$

and

$$
\begin{aligned}
&(\omega n j \| [c^{\dagger}_{p'} \tilde{c}_{n'}]_L \| p) \\
&\quad = -(-1)^{j_{p'}+j_{n'}+L}(-1)^{j_n+J_\omega-j}\hat{J}_\omega \hat{L}\hat{j}\left[\begin{Bmatrix} j_p & j & L \\ j_n & j_{p'} & J_\omega \end{Bmatrix}\right. \\
&\qquad \times \bar{X}^{\omega}_{pp'} v_{n'} u_{p'} \sigma^{-1}_{pp'} \delta_{nn'} (-1)^{j_p+j+L} \\
&\qquad \left. + \frac{\delta_{jj_{n'}}}{\hat{j}^2} \bar{Y}^{\omega}_{nn'} u_{n'} v_{p'} \sigma^{-1}_{nn'} \delta_{pp'} \right], \qquad (11)
\end{aligned}
$$

for transitions between one-quasiparticle and quasiparticle-phonon excitations. Here we have defined $\sigma_{aa'} = \sqrt{1+\delta_{aa'}}$ and $\bar{X}^{\omega}_{aa'} = X^{\omega}_{aa'} - (-1)^{j_a+j_{a'}-J_\omega} X^{\omega}_{a'a}$. For transitions between two quasiparticle-phonon excitations, one obtains

$$
\begin{aligned}
&(\omega n j \| [c^{\dagger}_{p'} \tilde{c}_{n'}]_L \| \omega' p j') \\
&\quad = -\left[(-1)^{j_p+J_\omega-j}\begin{Bmatrix} j & L & j' \\ j_{n'} & J_\omega & j_{p'} \end{Bmatrix}\delta_{pp'}\right. \\
&\qquad \times \left(\frac{1}{2}\delta_{nn'}\delta_{\omega\omega'} + K(n'\omega n\omega'; j')\right) \\
&\qquad + (-1)^{j_{p'}+J_{\omega'}-j}\begin{Bmatrix} j & L & j' \\ j_{n'} & J_{\omega'} & j_{p'} \end{Bmatrix}\delta_{nn'} \\
&\qquad \left. \times \left(\frac{1}{2}\delta_{pp'}\delta_{\omega\omega'} + K(p\omega p'\omega'; j)\right)\right] \\
&\qquad \times \hat{j}\hat{L}\hat{j}'(-1)^{j+L+j'} v_{p'} v_{n'} \\
&\qquad - \left[\begin{Bmatrix} j & L & j' \\ j_p & j_{p'} & J_{\omega'} \\ J_{\omega'} & j_{n'} & j_n \end{Bmatrix} \bar{X}^{\omega'}_{p'p} \bar{X}^{\omega}_{nn'} (-1)^{j_{n'}+j_{p'}-L}\right. \\
&\qquad \left. + \frac{\delta_{jj_{n'}}\delta_{j'j_{p'}}}{\hat{j}^2\hat{j}'^2} \bar{Y}^{\omega}_{pp'} \bar{Y}^{\omega'}_{n'n}\right] \sigma^{-1}_{nn'}\sigma^{-1}_{pp'}\hat{j}\hat{L}\hat{j}' \\
&\qquad \times (-1)^{j_p+J_\omega-j}\hat{J}_\omega \hat{J}_{\omega'} u_{p'} u_{n'}, \qquad (12)
\end{aligned}
$$

where

$$
\begin{aligned}
K(a\omega a'\omega'; j) = \hat{J}_\omega \hat{J}_{\omega'} \sum_b &\left[\begin{Bmatrix} j_{a'} & j_b & J_\omega \\ j_a & j & J_{\omega'} \end{Bmatrix} \bar{X}^{\omega}_{ba'} \bar{X}^{\omega'}_{ba}\right. \\
&\left. - \frac{\delta_{jj_b}}{\hat{j}^2} \bar{Y}^{\omega}_{ba} \bar{Y}^{\omega'}_{ba'}\right] \sigma^{-1}_{ba}\sigma^{-1}_{ba'} \qquad (13)
\end{aligned}
$$

and the matrix element $(\omega p j \| [c^{\dagger}_{p'} \tilde{c}_{n'}]_L \| \omega' n j')$ is obtained by making the substitution $u_a \to v_a$ and $v_a \to -u_a$.

B. Non-unique forbidden beta decay

The general formulation to calculate non-unique forbidden beta decays is provided in Ref. [8]. In this section this formulation is presented in a streamlined way allowing easy application to β^--decay calculations. Unlike in Ref. [8], where natural units were used, we will use SI units in this work.

When only the energy spectrum of the escaping electron is observed and the angular dependence has been integrated over, the probability of electron emission in the energy interval W_e to $W_e + dW_e$ is

$$
\begin{aligned}
P(W_e)dW_e = &\frac{G_{\mathrm{F}}^2}{(\hbar c)^6}\frac{1}{2\pi^3\hbar} C(W_e) p_e c W_e (W_0 - W_e)^2 \\
&\times F_0(Z, W_e) dW_e, \qquad (14)
\end{aligned}
$$

where $G_F/(\hbar c)^3$ is the Fermi coupling constant, $C(W_e)$ is the shape factor (discussed below), W_0 is the endpoint energy of the beta spectrum, and $F_0(Z, W_e)$ is the Fermi function. Furthermore, W_e is the energy and p_e the momentum of the emitted electron. The kinematical factors $p_e c W_e (W_0 - W_e)^2$ arise from the available phase space for the emitted electron and antineutrino. The half-life becomes then

$$
t_{1/2} = \frac{\ln 2}{\int_{m_e c^2}^{W_0} P(W_e) dW_e}, \qquad (15)
$$

where m_e is the mass of the electron.

The half-life of the decay can also be written in the form $t_{1/2} = \kappa/\tilde{C}$, where the constant

$$
\kappa = \frac{2\pi^3\hbar \ln 2}{(m_e c^2)^5 G_F^2/(\hbar c)^6} \qquad (16)
$$

has the value 6147s [17] and the unitless integrated shape factor is

$$
\tilde{C} = \int_1^{w_0} C(w_e) p w_e (w_0 - w_e)^2 F_0(Z, w_e) dw_e, \qquad (17)
$$

where the electron-mass scaled quantities are $w_0 = W_0/(m_e c^2)$, $w_e = W_e/(m_e c^2)$, $p = p_e c/(m_e c^2) = \sqrt{w_e^2 - 1}$, and $F_0(Z, w_e)$ is the Fermi function. The reduced half-life, or $\log ft$ value, is obtained by multiplying the half-life with the following unitless integrated Fermi function

$$
f = \int_1^{w_0} p w_e (w_0 - w_e)^2 F_0(Z, w_e) dw_e \qquad (18)
$$

and taking a base-10 logarithm.

The shape factor $C(w_e)$ can be obtained from [8]. It can be written in the form

$$
\begin{aligned}
C(w_e) = (6.706 \times 10^{-6})^K &\left[\sum_{k_e+k_\nu=K+1} \lambda_{k_e}\left(w_e^2 - 1\right)^{k_e-1}\right. \\
&\times (w_0 - w_e)^{2(k_\nu-1)} g_V^2 D^2_{K k_e k_\nu} \tilde{\mathcal{A}}_K \\
&+ \sum_{k_e+k_\nu=K+2} \lambda_{k_e}\left(w_e^2 - 1\right)^{k_e-1} \\
&\left. \times (w_0 - w_e)^{2(k_\nu-1)} g_V^2 \tilde{D}^2_{K k_e k_\nu} \mathcal{B}_K \right], \qquad (19)
\end{aligned}
$$

where k_e and k_ν are positive integers emerging from the partial wave expansion of the lepton wave functions. Their relation to the orbital angular momentum l of the leptons is

$$
k = \begin{cases} l & \text{for } j = l - \frac{1}{2} \\ l+1 & \text{for } j = l + \frac{1}{2}, \end{cases} \qquad (20)
$$

where j is the total angular momentum of the lepton, obtained by coupling the orbital angular momentum with the lepton spin.

Leading contributions to the shape factor come from the smallest possible electron (k_e) and neutrino (k_ν) partial waves satisfying $k_e + k_\nu = K + 1$ and $k_e + k_\nu = K + 2$ as indicated in (19). Hence, for the fourth-forbidden decay we have lepton orbital angular momenta corresponding up to $l_e, l_\nu \leqslant 6$ partial waves. In Eq. (19) we have used the scaling

$$6.706 \times 10^{-6} = \left(\frac{m_e c^2 \cdot \mathrm{fm}}{\hbar c}\right)^2 \tag{21}$$

by assuming that all the nuclear matrix elements in $\tilde{\mathcal{A}}_K$ and $\mathcal{B}_K$ are given in units of $(\mathrm{fm})^K$.

The quantities $\tilde{\mathcal{A}}_K$ and $\mathcal{B}_K$ can be expressed in terms of kinematical factors and nuclear form factors $F_{KLS}(q^2)$ [8], where K is the multipolarity of the involved transition operator. The form factors can be related to the nuclear matrix elements for small momentum exchange q^2 in the impulse approximation. In this case the most important contribution to the decay rate will arise from the form factors that are related to the minimal transferred angular momentum. Order-of-magnitude considerations done in Ref. [8] imply that the following four form factors:

$$^{V}F^{(0)}_{K,K-1,1}, \quad ^{V}F^{(0)}_{KK0}, \quad ^{A}F^{(0)}_{KK1}, \quad ^{A}F^{(0)}_{K+1,K1} \tag{22}$$

will be the most important when calculating the beta decay rate. Above we have denoted

$$^{V/A}F^{(0)}_{KLS} \equiv {}^{V/A}F_{KLS}(q^2 = 0). \tag{23}$$

In order to express the form factors $^{V/A}F^{(0)}_{KLS}$ in terms of nuclear matrix elements we use the impulse approximation [8]. This leads to

$$R^L {}^{V}F^{(0)}_{KLS} \to (-1)^{K-L} g_V {}^{V}\mathcal{M}^{(0)}_{KLS} \tag{24a}$$

and

$$R^L {}^{A}F^{(0)}_{KLS} \to (-1)^{K-L+1} g_A {}^{A}\mathcal{M}^{(0)}_{KLS}, \tag{24b}$$

where R is the nuclear radius. We define the following matrix elements for a fixed multipolarity K:

$$R^{K-1} {}^{V}F^{(0)}_{K,K-1,1} \to -g_V {}^{V}\mathcal{M}^{(0)}_{K,K-1,1} \equiv -g_V M_1, \tag{24c}$$

$$R^K {}^{V}F^{(0)}_{KK0} \to g_V {}^{V}\mathcal{M}^{(0)}_{KK0} \equiv g_V M_2, \tag{24d}$$

$$R^K {}^{A}F^{(0)}_{KK1} \to -g_A {}^{A}\mathcal{M}^{(0)}_{KK1} \equiv -g_A M_3, \tag{24e}$$

$$R^K {}^{A}F^{(0)}_{K+1,K1} \to g_A {}^{A}\mathcal{M}^{(0)}_{K+1,K1} \equiv g_A M_4, \tag{24f}$$

$$R^K {}^{V}F^{(0)}_{KK0}(k_e, 1, 1, 1) \to g_V {}^{V}\mathcal{M}^{(0)}_{KK0}(k_e, 1, 1, 1) \equiv g_V M_2^{(k_e)}, \tag{24g}$$

$$R^K {}^{A}F^{(0)}_{KK1}(k_e, 1, 1, 1) \to -g_A {}^{A}\mathcal{M}^{(0)}_{KK1}(k_e, 1, 1, 1) \equiv -g_A M_3^{(k_e)}. \tag{24h}$$

For convenience, we adopt the linear combinations

$$M_\pm = M_2 \pm \sqrt{\frac{K+1}{K}}\frac{g_A}{g_V} M_3 \tag{25}$$

and

$$M_-^{(k_e)} = M_2^{(k_e)} - \sqrt{\frac{K+1}{K}}\frac{g_A}{g_V} M_3^{(k_e)}. \tag{26}$$

The factors containing the nuclear matrix elements are then given by

$$\begin{aligned}
\tilde{\mathcal{A}}_K = {} & \frac{2K+1}{K}\tilde{M}_1^2 + \frac{1}{(2k_e+1)^2}\big[(\tilde{\alpha}Z)^2 (M_-^{(k_e)})^2 \\
& + 2(\tilde{\alpha}Z) w_e M_- M_-^{(k_e)} + \big(1 + w_e^2\big) M_-^2\big] \\
& - \frac{2\gamma_{k_e}}{k_e w_e (2k_e+1)^2}[(\tilde{\alpha}Z) M_- M_-^{(k_e)} + w_e M_-^2] \\
& + \frac{1}{(2k_\nu+1)^2}(w_0 - w_e)^2 M_+^2 \\
& - \frac{2}{2k_e+1}\sqrt{\frac{2K+1}{K}}[(\tilde{\alpha}Z)\tilde{M}_1 M_-^{(k_e)} + w_e \tilde{M}_1 M_-] \\
& + \frac{2}{2k_e+1}\sqrt{\frac{2K+1}{K}}\frac{\gamma_{k_e}}{k_e w_e}\tilde{M}_1 M_- \\
& - \frac{2}{2k_\nu+1}\sqrt{\frac{2K+1}{K}}(w_0 - w_e)\tilde{M}_1 M_+ \\
& + \frac{2}{(2k_e+1)(2k_\nu+1)}(w_0 - w_e) \\
& \times [(\tilde{\alpha}Z) M_-^{(k_e)} + w_e M_-] M_+ \\
& - \frac{2}{(2k_e+1)(2k_\nu+1)}\frac{\gamma_{k_e}}{k_e w_e}(w_0 - w_e) M_- M_+
\end{aligned} \tag{27}$$

and

$$\begin{aligned}
\mathcal{B}_K = {} & \frac{K+1}{(2k_e-1)(2k_\nu-1)}\left[M_2^2 + 2\frac{g_A}{g_V}\frac{k_e - k_\nu}{\sqrt{K(K+1)}} M_2 M_3 \right. \\
& \left. + \frac{(k_e - k_\nu)^2}{K(K+1)}\left(\frac{g_A}{g_V}\right)^2 M_3^2\right] + \left(\frac{g_A}{g_V}\right)^2 M_4^2.
\end{aligned} \tag{28}$$

Here g_V and g_A are the usual vector and axial-vector coupling constants.

In Eq. (19) we have defined according to [8]

$$D_{Kk_e k_\nu} = \frac{1}{\sqrt{2}}\sqrt{\frac{(2K)!!}{(2K+1)!!}}\frac{1}{\sqrt{(2k_e-1)!(2k_\nu-1)!}}, \tag{29}$$

$$\tilde{D}_{Kk_e k_\nu} = \sqrt{\frac{(2K)!!}{(2K+1)!!}}\frac{1}{\sqrt{(2k_e-1)!(2k_\nu-1)!}}, \tag{30}$$

and

$$\lambda_{k_e} = \frac{F_{k_e-1}(Z, w_e)}{F_0(Z, w_e)}. \tag{31}$$

The quantity $F_{k_e-1}(Z, w_e)$ is the generalized Fermi function [8]

$$F_{k_e-1}(Z, w_e) = 4^{k_e-1}(2k_e)(k_e + \gamma_{k_e})[(2k_e - 1)!!]^2 \times e^{\pi y}\left(\frac{2p_eR}{\hbar}\right)^{2(\gamma_{k_e}-k_e)} \times \left(\frac{|\Gamma(\gamma_{k_e} + iy)|}{\Gamma(1 + 2\gamma_{k_e})}\right)^2, \quad (32)$$

where $y = (\alpha Z w_e)/(p_e c)$. The dimensionless factors γ_{k_e} and $\tilde{\alpha}$ in Eq. (27) read

$$\gamma_{k_e} = \sqrt{k_e^2 - (\alpha Z)^2} \quad (33)$$

and

$$\tilde{\alpha} = \frac{\alpha\hbar}{Rm_e c}. \quad (34)$$

The scaled matrix element

$$\tilde{M}_1 = \frac{\hbar c}{m_e c^2} M_1 = 386.2\,\text{fm} \times M_1 \quad (35)$$

has been defined in Eq. (27) in order that all the matrix elements $\tilde{M}_1$, M_2, M_3, and M_4 in Eq. (24) have the units $(\text{fm})^K$. When expressed in these units the numerical values of the matrix elements $\tilde{M}_1$ and $M_2 - M_4$ can be inserted in the quantities $\tilde{\mathcal{A}}_K$ and $\mathcal{B}_K$ of Eqs. (27) and (28). Then the remaining scaling factor $(\text{fm})^{2K}$ of the squared matrix elements goes into the numerical factor (21), raised to the power K in Eq. (19).

The needed nuclear matrix elements can be calculated from the expression

$${}^{V/A}\mathcal{M}^{(0)}_{KLS} = \frac{1}{\sqrt{2J_i + 1}} \sum_{pn} {}^{V/A}m_{KLS}(pn) \times (\psi_f \| [c_p^\dagger \tilde{c}_n]_K \| \psi_i), \quad (36)$$

where the single-particle transition densities $(\psi_f \| [c_p^\dagger \tilde{c}_n]_K \| \psi_i)$ are obtained from the nuclear wave functions ψ_f and ψ_i, i.e., from the nuclear model. The involved single-particle transition matrix elements ${}^{V/A}m_{KLS}(pn)$ are given by

$${}^{V}m_{KLS}(pn) = \frac{1}{\sqrt{2K + 1}}(p \| T_{KLS} \| n), \quad (37)$$

$${}^{A}m_{KLS}(pn) = \frac{1}{\sqrt{2K + 1}}(p \| \gamma_5 T_{KLS} \| n). \quad (38)$$

The transition operator T_{KLS} is given in the spherical tensor notation as

$$T_{KLSM} = \begin{cases} i^L r^L Y_{LM} \delta_{LK}, & S = 0, \\ i^L (-1)^{L+1-K} r^L [Y_L \sigma]_{KM}, & S = 1, \end{cases} \quad (39)$$

where Y_{LM} is the usual spherical harmonic and σ the Pauli spin operator.

To evaluate the single-particle matrix elements we use the relativistic single-particle spinor wave function

$$\phi_{nljm}(\mathbf{r}) = \begin{pmatrix} G_{nljm}(\mathbf{r}) \\ F_{nljm}(\mathbf{r}), \end{pmatrix} \quad (40)$$

where the large component G_{nljm} is taken to be a solution of the non-relativistic Schrödinger equation. These solutions are written in the form.

$$G_{nljm}(\mathbf{r}) = i^l g_{nl}(r)[Y_l \chi_{\frac{1}{2}}]_{jm}, \quad (41)$$

where $\chi_{\frac{1}{2}m_s}$ is the nonrelativistic spin-$\frac{1}{2}$ spinor. The small component of the spinor wave function (40) is

$$F_{nljm}(\mathbf{r}) = \frac{\boldsymbol{\sigma} \cdot \mathbf{p}}{2M_N c} G_{nljm}(\mathbf{r}), \quad (42)$$

where M_N is the nucleon mass and $\mathbf{p}$ its momentum, to be interpreted as a derivative operator. Taking $g_{nl}(r)$ to be harmonic-oscillator wave functions the small component can be evaluated analytically. The result for $j = 1 \pm \frac{1}{2}$ is

$$F_{nljm}(\mathbf{r}) = \frac{i^{l+1}\hbar}{2(M_N c)b}(-1)^{l+j-\frac{1}{2}}\left(\frac{r}{b} g_{nl} - 2\sqrt{n + j + 1}\, g_{n,l\pm1}\right)[Y_{l\pm1}\chi_{\frac{1}{2}}]_{jm}, \quad (43)$$

where b is the harmonic-oscillator size parameter.

In terms of the large and small components of Eq. (40) the involved single-particle matrix elements can be written as

$${}^{V}m_{KK0}(pn) = \frac{1}{\sqrt{2K + 1}}[(G_p \| T_{KK0} \| G_n) + (F_p \| T_{KK0} \| F_n)], \quad (44a)$$

$${}^{A}m_{KL1}(pn) = \frac{1}{\sqrt{2K + 1}}[(G_p \| T_{KL1} \| G_n) + (F_p \| T_{KL1} \| F_n)], \quad (44b)$$

and

$${}^{V}m_{KL1}(pn) = \frac{1}{\sqrt{2K + 1}}[(G_p \| T_{KL1} \| F_n) + (F_p \| T_{KL1} \| G_n)]. \quad (44c)$$

After some algebra the matrix elements can be rewritten as

$${}^{V}m_{KK0}(pn) = i^{l_p+l_n+K}\frac{1 + (-1)^{l_p+l_n+K}}{2} \times (-1)^{j_p+j_n+1}\frac{\hat{j}_p\hat{j}_n}{\hat{K}}\left(j_p\ \tfrac{1}{2}\ j_n\ -\tfrac{1}{2}\middle|K\ 0\right) \times \left[(-1)^{l_n+j_n-1/2}\langle r^K\rangle_{pn}\Delta(l_p l_n K) + (-1)^{l_p+j_p-1/2}\{r^K\}_{\tilde{p}\tilde{n}}\Delta(\tilde{l}_p\tilde{l}_n K)\right], \quad (45a)$$

$${}^{A}m_{KL1}(pn) = i^{l_p+l_n+L}(-1)^{K+1}\frac{\hat{L}\hat{j}_p\hat{j}_n}{\hat{K}}\frac{1 + (-1)^{l_p+l_n+L}}{2} \times \left(j_p\ \tfrac{1}{2}\ j_n\ -\tfrac{1}{2}\middle|K\ 0\right)\left\{[\mathcal{A}_{KL}(pn) + \mathcal{B}_{KL}(pn)]\langle r^L\rangle_{pn}\Delta(l_p l_n L) + (-1)^{l_p+l_n+j_p+j_n}[\mathcal{A}_{KL}(pn) - \mathcal{B}_{KL}(pn)]\{r^L\}_{\tilde{p}\tilde{n}}\Delta(\tilde{l}_p\tilde{l}_n L)\right\}, \quad (45b)$$

and

$$
\begin{aligned}
{}^{V}m_{KL1}(pn) = i^{l_p+l_n+L+1}\frac{1+(-1)^{l_p+l_n+L+1}}{2}\frac{\hat{L}\hat{j}_p\hat{j}_n}{\hat{K}} \\
\times \left(j_p\ \tfrac{1}{2}\ j_n\ -\tfrac{1}{2}|K\ 0\right) \\
\times \big\{[\mathcal{A}_{KL}(pn)+\mathcal{B}_{KL}(pn)](-1)^{K+l_n+j_n+1/2} \\
\times \{r^L\}_{p\tilde{n}}\Delta(l_p\tilde{l}_nL) \\
+[\mathcal{A}_{KL}(pn)-\mathcal{B}_{KL}(pn)](-1)^{K+l_p+j_p+1/2} \\
\times \{r^L\}_{\tilde{p}n}\Delta(\tilde{l}_pl_nL)\big\}. \qquad (45c)
\end{aligned}
$$

Above $\Delta(l_1l_2L)$ denotes the triangular condition for the coupling of the angular momenta l_1, l_2, and L. Furthermore, the geometric factors are

$$
\begin{aligned}
\mathcal{A}_{KL}(pn) = \frac{\hat{j}_p^2+(-1)^{j_p+j_n+K}\hat{j}_n^2}{\sqrt{2K(K+1)(2L+1)}}(-1)^{K+1} \\
\times (K11-1|L0)(1-\delta_{K0}), \qquad (46)
\end{aligned}
$$

$$
\mathcal{B}_{KL}(pn) = (-1)^{l_p+j_p-1/2+K}\hat{L}^{-1}(K\ 0\ 1\ 0|L\ 0), \qquad (47)
$$

and the auxiliary orbital angular-momentum quantum number has been defined as

$$
\tilde{l} = \begin{cases} l+1, & j = l+\frac{1}{2}, \\ l-1, & j = l-\frac{1}{2}. \end{cases} \qquad (48)
$$

The involved radial factors are defined as

$$
\{r^L\}_{p\tilde{n}} = k(b)\left(b^{-1}\langle r^{L+1}\rangle_{pn} - 2\sqrt{n_n+j_n+1}\langle r^L\rangle_{p\tilde{n}}\right), \qquad (49a)
$$

$$
\{r^L\}_{\tilde{p}n} = k(b)\left(b^{-1}\langle r^{L+1}\rangle_{pn} - 2\sqrt{n_p+j_p+1}\langle r^L\rangle_{\tilde{p}n}\right), \qquad (49b)
$$

and

$$
\begin{aligned}
\{r^L\}_{\tilde{p}\tilde{n}} = k(b)^2\Big(b^{-2}\langle r^{L+2}\rangle_{pn}2b^{-1}\sqrt{n_p+j_p+1}\langle r^{L+1}\rangle_{\tilde{p}n} \\
-2b^{-1}\sqrt{n_n+j_n+1}\langle r^{L+1}\rangle_{p\tilde{n}} \\
+4\sqrt{(n_p+j_p+1)(n_n+j_n+1)}\langle r^L\rangle_{\tilde{p}\tilde{n}}\Big), \qquad (49c)
\end{aligned}
$$

where the basic radial integral reads

$$
\langle r^L\rangle_{pn} = \int_0^\infty g_{n_pl_p}(r)r^L g_{n_nl_n}r^2dr. \qquad (50)
$$

Here the notation $\tilde{p}$ ($\tilde{n}$) has to be understood as a set of quantum numbers $\tilde{p} = n_p\tilde{l}_pj_p$ ($\tilde{n} = n_n\tilde{l}_nj_n$). The involved auxiliary quantity has been defined as

$$
k(b) = \frac{1}{2M_nb} = \frac{0.1051}{b\,[\mathrm{fm}]}, \qquad (51)
$$

where in the last, numerical expression the harmonic oscillator parameter

$$
b = \frac{197.33}{\sqrt{939\hbar\omega}}\ \mathrm{fm}, \qquad \hbar\omega = 45A^{-1/3}-25A^{-2/3}, \qquad (52)
$$

has been expressed in units of fm. When the basic radial integral (50) is expressed as $(\mathrm{fm})^L$ then all the single-particle matrix elements (45a)–(45c) have the dimension $(\mathrm{fm})^L$.

The k_e dependent matrix elements $M_2^{(k_e)}$ and $M_3^{(k_e)}$ are calculated just like M_2 and M_3 except that the Coulomb factor

$$
I(k_e,1,1,1;r) = \begin{cases} \frac{3}{2}-\frac{2k_e+1}{2(2k_e+3)}\left(\frac{r}{R}\right)^2, & 0\leqslant r\leqslant R \\ \frac{2k_e+1}{2k_e}\frac{R}{r}-\frac{3}{2k_e(2k_e+3)}\left(\frac{R}{r}\right)^{2k_e+1}, & r>R \end{cases} \qquad (53)
$$

is appended to the integrand of the radial integral (50).

From the single-particle matrix elements of Eqs. (45a)–(45c) we can write our final matrix elements M_1–M_4 as

$$
M_1 = \hat{J}_i^{-1}\sum_{pn}{}^{V}m_{K,K-1,1}(pn)(\psi_f\|[c_p^\dagger\tilde{c}_n]_K\|\psi_i), \qquad (54a)
$$

$$
M_2 = \hat{J}_i^{-1}\sum_{pn}{}^{V}m_{KK0}(pn)(\psi_f\|[c_p^\dagger\tilde{c}_n]_K\|\psi_i), \qquad (54b)
$$

$$
M_3 = \hat{J}_i^{-1}\sum_{pn}{}^{A}m_{KK1}(pn)(\psi_f\|[c_p^\dagger\tilde{c}_n]_K\|\psi_i), \qquad (54c)
$$

and

$$
M_4 = \hat{J}_i^{-1}\sum_{pn}{}^{A}m_{K+1,K1}(pn)(\psi_f\|[c_p^\dagger\tilde{c}_n]_{K+1}\|\psi_i). \qquad (54d)
$$

III. NUMERICAL APPLICATION

The mean-field single-particle states were generated by a coulomb-corrected Woods-Saxon (WS) potential with the parametrization of Bohr and Mottelson [18]. The adopted valence space consisted of the $3\hbar\omega$ and $4\hbar\omega$ oscillator major shells augmented by the $0h$ states from the $5\hbar\omega$ major shell. Slight modifications (see Table I) were made to some of the WS single-particle energies. In this way the resulting BCS quasiparticle spectra for protons and neutrons would better correspond to those experimental low-energy states in the adjacent proton-odd and neutron-odd nuclei that could be reasonably assumed to be dominantly of one-quasiparticle character. The two-body interaction matrix elements used throughout the calculations were generated from the Bonn one-boson-exchange potential applying G-matrix techniques [19].

The interaction matrix elements involved in the BCS calculations were scaled by a constant $g_{\mathrm{pair}}^{(p)}$ for the protons

TABLE I. Woods-Saxon energies and the manually adjusted energies in units of MeV. The proton and neutron orbitals are denoted with π and ν, respectively.

Nucleus	Orbital	Woods-Saxon	Adjusted
^{112}Cd	$\pi 1p_{3/2}$	−11.14	−10.0
	$\pi 0g_{9/2}$	−8.57	−9.4
	$\nu 0g_{7/2}$	−8.66	−9.5
	$\nu 0h_{11/2}$	−6.04	−7.1
^{116}Sn	$\pi 1p_{1/2}$	−9.58	−8.8
	$\pi 1p_{3/2}$	−11.10	−9.4
	$\nu 1d_{3/2}$	−7.74	−7.4
	$\nu 0h_{11/2}$	−6.83	−7.2

and $g_{\rm pair}^{(n)}$ for the neutrons, so that the phenomenological proton and neutron pairing gaps were reproduced. The pairing gaps were calculated by Eqs. (4a) and (4b) using the experimental separation energies from Refs. [6,7,20–23]. The following values for the scaling constants were obtained: for ^{112}Cd $g_{\rm pair}^{(p)} = 1.02$ and $g_{\rm pair}^{(n)} = 0.93$, and for ^{116}Sn $g_{\rm pair}^{(p)} = 1.13$ and $g_{\rm pair}^{(n)} = 0.94$. Hence the scaling needed was quite small, indicating that the monopole part of the used G-matrix is, as such, suitable for pairing calculations.

The quasiparticle energy spectra were quite succesful in reproducing the low-energy spectra of the relevant odd-mass nuclei in all the cases except ^{113}Cd. In the case of ^{116}Sn, due to the magic proton number $Z = 50$ and the fact that the isotope ^{115}In was to be modeled using this reference nucleus, a proton number $Z = 48$ had to be used instead to achieve a reasonable quasiparticle energy spectrum for protons. Without this little trick, no reasonable ordering of the one-quasiparticle states could be achieved. The proton-quasiparticle spectrum for $Z = 50$ would have, however, nicely agreed with the low-energy spectrum of ^{117}Sb.

In the QRPA calculations the interaction matrix elements were scaled separately for each multipole, as tabulated in Table II. The scaling constants were taken to be $g_{\rm ph}$ for the particle-hole part and $g_{\rm pp}$ for the particle-particle part of the proton-neutron residual interaction, as discussed in Ref. [24]. In this way the lowest excitation energy of each multipole was brought as close to the experimental energy as possible. If this was not possible with a reasonable scaling, then a more complex structure of the state was assumed and the scaling constant was taken to be 1 in default of any better alternative.

The $0^+, 2^+$, and 4^+ triplet of excited states around 1.3 MeV was ignored when doing the QRPA calculation for ^{112}Cd because of their known two-phonon nature [25], which is obviously beyond the scope of the QRPA.

As the final step, the MQPM calculations were performed for the beta-decay mother and daughter nuclei starting from the same even-even reference nucleus. The number of the QRPA phonons used was increased until there was no notable effect on the low-energy spectra of the involved odd-mass nuclei. Finally, four 2^+ and two 4^+, 5^- and 6^+ in addition to one 1^-, 3^-, and 7^- QRPA phonons were used in the MQPM calculation for the $A = 113$ nuclei. Similarly, six 2^+, 3^-, 4^+, and 5^-, as well as four 1^- phonons were used for the $A = 115$ nuclei. The final MQPM spectra, and their comparison to the experimental low-energy spectra of the involved odd-mass nuclei, are presented in Fig. 2.

As seen in Fig. 2, the MQPM was unable to exactly reproduce the ordering of the low-energy states of ^{113}Cd. This traces all the way back to the BCS quasiparticle spectrum, where the attempts to improve the ordering of the computed single-quasiparticle spectrum by slight adjustments to the single-particle energies failed. However, it is reasonable to expect that this has little effect on the ground-state wave function.

Interestingly, in the MQPM spectrum for ^{113}In there are plenty of low-energy states not seen in the experimental spectrum. In most of these states the dominant component is $2_1^+ \otimes 0g_{9/2}$. The fact that these states push themselves so low in the MQPM spectrum reduces slightly the dominance of the $0g_{9/2}$ one-quasiparticle state in the ground-state wave function. Consequently, this may partially explain why the calculated decay rate is slower than the corresponding experimental one.

In the MQPM spectrum of ^{115}Sn the ordering of the $\frac{7}{2}_1^+$ and $\frac{11}{2}_1^-$ is reversed relative to the experiment. The MQPM spectrum of ^{115}In, on the other hand, seems to agree with the experimental one rather nicely, even if the density of states above 800 keV of excitation energy is lower in the MQPM spectrum. This is natural, since the excitations of five and more quasiparticles are absent from the MQPM.

Once the MQPM description of the nuclei was complete, the resulting wave functions were used to compute the charge-changing transition densities needed in the beta-decay-rate calculations. It was observed that, unsurprisingly, the transition densities (^{113}In; $\frac{9}{2}^+_{\rm g.s.} \| [c^\dagger_{\pi 0g_{9/2}} \tilde{c}_{\nu 2s_{1/2}}]_{4,5} \| ^{113}$Cd; $\frac{1}{2}^+_{\rm g.s.}$) and (^{115}Sn; $\frac{1}{2}^+_{\rm g.s.} \| [c^\dagger_{\pi 2s_{1/2}} \tilde{c}_{\nu 0g_{9/2}}]_{4,5} \| ^{115}$In; $\frac{1}{2}^+_{\rm g.s.}$) were clearly dominant in the corresponding decays. The nuclear matrix elements, the $\log ft$ values, and the half-lives were then calculated utilizing the formulas presented in Sec. II B. The obtained nuclear matrix elements are listed in Table III.

TABLE II. Values of the interaction scaling constants used in the QRPA calculations: $g_{\rm ph}$ is the scaling constant for the particle-hole and $g_{\rm pp}$ for the particle-particle interaction matrix elements. The blank voids denote the default value 1.

J^π	^{112}Cd		^{116}Sn	
	$g_{\rm ph}$	$g_{\rm pp}$	$g_{\rm ph}$	$g_{\rm pp}$
0^+	1.07	0.87	0.78	0.86
1^-	0.52		0.48	
2^+	0.71		0.62	
3^-	0.72		0.75	
4^+	0.89		0.66	
5^-	0.82		0.56	
6^+	0.39			
7^-	1.05			

TABLE III. Calculated beta-decay nuclear matrix elements in units of fm^4.

	^{113}Cd $\rightarrow$ ^{113}In	^{115}In $\rightarrow$ ^{115}Sn
$\tilde{M}_1$	2.6313	5.8251
M_2	596.51	−554.77
M_3	532.99	−477.23
M_4	876.49	832.43
$M_2^{(1)}$	655.96	−612.25
$M_2^{(2)}$	612.71	−572.37
$M_2^{(3)}$	589.52	−550.97
$M_2^{(4)}$	575.23	−537.77
$M_3^{(1)}$	586.88	−527.15
$M_3^{(2)}$	548.36	−492.92
$M_3^{(3)}$	527.70	−474.53
$M_3^{(4)}$	514.96	−463.19

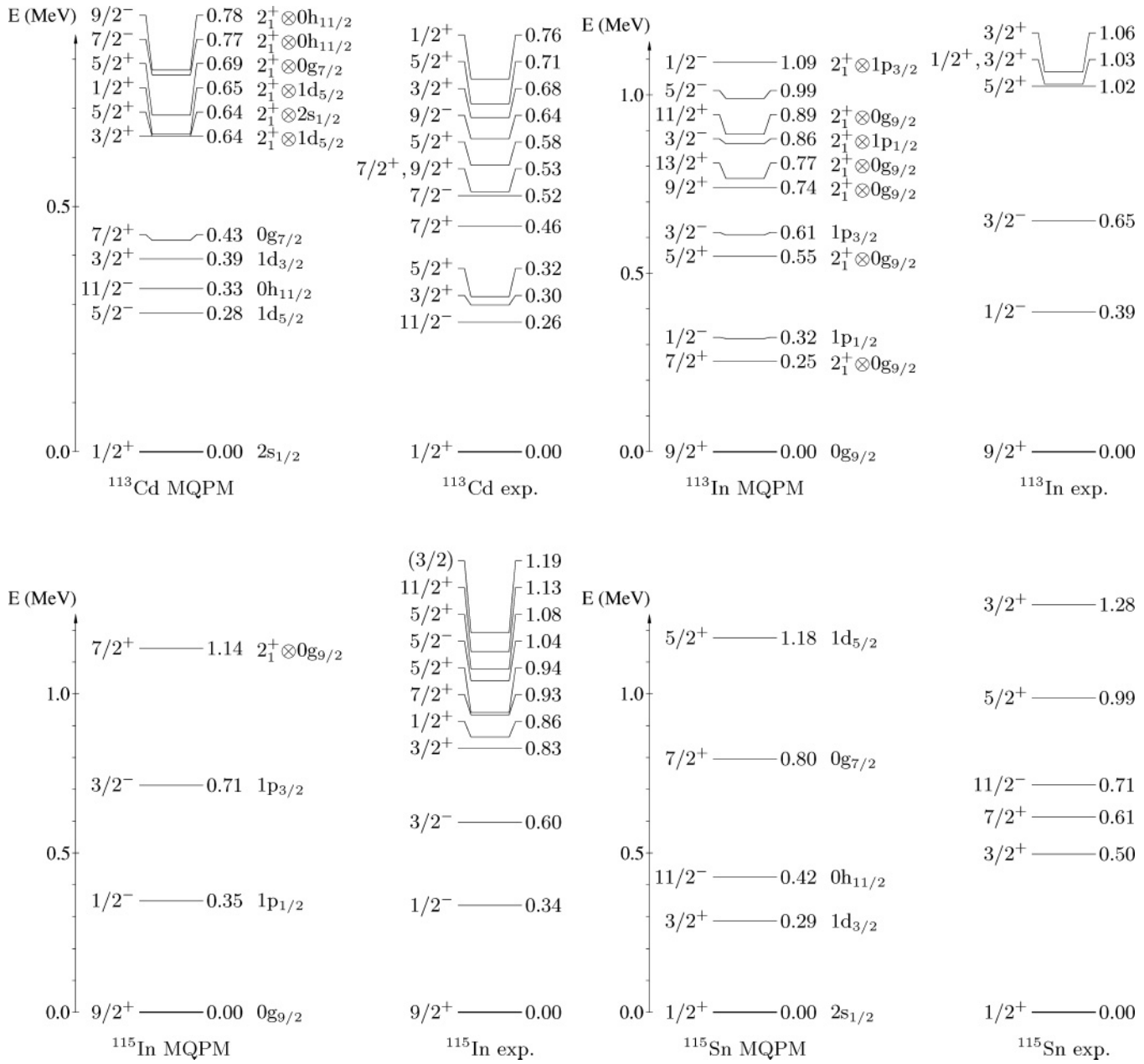

FIG. 2. Comparison between the MQPM spectra and the experimental low-energy spectra of the nuclei ^{113}Cd, ^{113}In, ^{115}In, and ^{115}Sn. The spin-parity of the state is indicated on the left of the level, whereas the excitation energy on the right of the level. For the theoretical spectrum also the main component of the wave function of the state is given on the right.

The computed log ft values 23.94 and 23.20 were obtained for the ground-state-to-ground-state decays of ^{113}Cd and ^{115}In, respectively. The corresponding experimental values [6,7] are 23.20(10) and 22.5, respectively. This implies that the transitions are somewhat faster in reality than obtained by the MQPM. However, the difference is not very large and the trend of the log ft values is correctly reproduced.

The half-lives calculated from the obtained log ft values were 4.95×10^{16} yrs for the decay of ^{113}Cd and 1.99×10^{15} yrs for the decay of ^{115}In. The corresponding experimental values are $7.7(3) \times 10^{15}$ yrs and $4.41(25) \times 10^{14}$ yrs, respectively. The recent measurement for ^{113}Cd [1] gives $(8.2 \pm 0.2(\text{stat.})^{+0.2}_{-1.0}(\text{sys.})) \times 10^{15}$ yrs.

IV. SUMMARY AND CONCLUSIONS

The mother and daughter nuclei of the fourth-forbidden non-unique beta decays of ^{113}Cd and ^{115}In were modelled using the microscopic quasiparticle-phonon model. The resulting low-energy excitation spectra of the involved mother and daughter nuclei corresponded rather well to the experimental spectra. This was considered as a test of the theoretical

framework since only the composition of the wave functions of the ground states of the involved nuclei were of interest to us.

The computed ground-state wave functions were used to calculate the required transition densities for evaluation of the beta-decay half-lives and log ft values of the discussed transitions. In this step we applied the Behrens and Bühring formulation of the β^- decay amplitudes for non-unique forbidden transitions.

According to the available experimental data, the transitions seem to be faster than what was predicted by the calculations. The difference between the experimental and theoretical values is, however, not as large as one could expect considering previous calculations [9] for the allowed beta decays in some medium-mass and heavy nuclei.

ACKNOWLEDGMENTS

This work was supported by the Academy of Finland under the Finnish Center of Excellence Program 2006-2011 (Nuclear and Accelerator Based Program at JYFL).

[1] C. Goeßling, M. Junker, H. Kiel, D. Muenstermann, S. Oehl, and K. Zuber, Phys. Rev. C **72**, 064328 (2005).
[2] J. Suhonen and O. Civitarese, Phys. Rep. **300**, 123 (1998).
[3] M. Aunola, J. Suhonen, and T. Siiskonen, Europhys. Lett. **46**, 577 (1999).
[4] J. Toivanen and J. Suhonen, J. Phys. G **21**, 1491 (1995); Phys. Rev. C **57**, 1237 (1998).
[5] J. Suhonen, J. Toivanen, A. Holt, T. Engeland, E. Osnes, and M. Hjorth-Jensen, Nucl. Phys. **A628**, 41 (1998).
[6] J. Blachot, Nucl. Data Sheets **107**, 791 (2005).
[7] J. Blachot, Nucl. Data Sheets **104**, 967 (2005).
[8] H. Behrens and W. Bühring, *Electron Radial Wave Functions and Nuclear Beta-Decay* (Clarendon, Oxford, 1982).
[9] E. Holmlund and J. Suhonen, Nucl. Phys. **A706**, 335 (2002).
[10] J. Suhonen, Nucl. Phys. **A563**, 205 (1993).
[11] M. Bertschy, S. Drissi, P. E. Garrett, J. Jolie, J. Kern, S. J. Mannanal, J. P. Vorlet, N. Warr, and J. Suhonen, Phys. Rev. C **51**, 103 (1995).
[12] M. Aunola and J. Suhonen, Nucl. Phys. **A602**, 133 (1996).
[13] A. Bohr, B. R. Mottelson, and D. Pines, Phys. Rev. **110**, 936 (1958).
[14] M. Baranger, Phys. Rev. **120**, 957 (1960).
[15] K. L. G. Heyde, *The Nuclear Shell Model*, 2nd ed. (Springer-Verlag, Berlin, 1994).
[16] D. J. Rowe, Rev. Mod. Phys. **40**, 153 (1968).
[17] J. Hardy, I. Towner, V. Koslowsky, E. Hagberg, and H. Schmeing, Nucl. Phys. **A509**, 429 (1990).
[18] A. Bohr and B. R. Mottelson, *Nuclear Structure*, Vol. I (W. A. Benjamin, New York, 1969).
[19] K. Holinde, Phys. Rep. **68**, 121 (1981).
[20] J. Blachot, Nucl. Data Sheets **100**, 179 (2003).
[21] D. De Frenne and E. Jacobs, Nucl. Data Sheets **79**, 639 (1996).
[22] J. Blachot, Nucl. Data Sheets **92**, 455 (2001).
[23] J. Blachot, Nucl. Data Sheets **95**, 679 (2002).
[24] J. Suhonen, T. Taigel, and A. Faessler, Nucl. Phys. **A486**, 91 (1988).
[25] J. Kotila, J. Suhonen, and D. S. Delion, Phys. Rev. C **68**, 014307 (2003).